

## Corrosion behavior in model solutions of steels suggested as construction materials for mining industries

D. I. Ivanova\*, G. P. Ilieva, L. B. Fachikov

University of Chemical Technology and Metallurgy, 8 "Kliment Ohridski" Blvd., 1756 Sofia, Bulgaria

Received November 15, 2017; Accepted December 12, 2017

A comparative study concerning corrosion behaviours of two steels suggested as construction materials in mining industries have been carried out. Samples of widely used carbon steel st.25 and the new conceived, low-alloyed, steel KP-355 (0.96 % Cr, 0.36 % Cu) have been tested. The tests have been held in model media containing the main aggressive components appearing in real mining waste waters. The main parameters characterizing the mechanical and corrosion-electrochemical behaviour of the tested materials have been determined by physical and electrochemical methods. It has been estimated that the steel KP-355 exhibited better mechanical strength behaviour and higher corrosion resistance in all media used in the tests.

**Key words:** corrosion, carbon and low-alloyed steels, mine waters.

### INTRODUCTION

The working conditions in mines are characterized by high aggressive behaviour of underground waters and gases with respect to the metallic equipment used. The aggressive components in such media are mainly dissolved salts, dominantly chlorides and sulphates and to some extent nitrates and carbonates and dissolved gases (mainly oxygen). In addition, contaminants such as mechanical pollutants, animal and plant related microorganisms also are present. The quantities and type of all aforementioned contaminants is mainly dependent on the soil content, temperatures and flow rates of underground waters. The underground waters are mainly neutral or close to this state, but there are also with acid and basic reaction behaviours [1-4].

The mining atmospheres are characterized with high humidity and contain dangerous contaminants related to the corrosion aggression such as sulphur oxides, hydrogen sulphide, carbon and nitrogen oxides, etc. Moreover, solid particles (such as corrosion active salts NaCl, Na<sub>2</sub>SO<sub>4</sub>; various natural adsorbents; inert sands and product of blasts) are also present in both gases and waters in mining environments. Most of these contaminants are natural (depending on the soil content) whereas others are results of detonates and other mining operations [2-3].

The alloying components used in the low-alloyed steels are related to enhancement of their mechanical characteristics. In this context, replace the carbon steels when elements of equipment working under high mechanical loads are at issue or

low-weight parts are needed. Moreover, carbon steels alloyed by copper (0.2-0.8 %) or by copper and chrome (1-2 %), with high corrosion resistances are of primary practical importance. They are well applicable in metal constructions with welded parts, working in environments of sea waters, high mineralized industrial wastewaters, etc. [5-9].

The corrosion of carbon and low-alloyed steels in mine waters or model solutions is intensively studied. The corrosion kinetics in aerated, neutral solutions of chlorides (Cl<sup>-</sup> > 1.5 %) has been investigated by electrochemical methods [10, 11], whereas the impedance method has been applied in [12].

The corrosion behaviour of low-alloyed steels in mining waters and in 3 % NaCl solutions (with flow rate of 2 m s<sup>-1</sup> at 20-55°C) has been studied in [13]. It has been estimated that in mining waters the main corrosion products are α-FeOOH, γ-FeOOH and Fe<sub>3</sub>O<sub>4</sub>, whereas in the chloride solution they are - α-FeOOH, β-FeOOH, α-Fe<sub>2</sub>O<sub>3</sub> γ-FeOOH.

In this work results on corrosion behaviour of two steels suggested for metal mining propping is reported. Samples of widely used carbon steel st.25 and a newly suggested KP-355 have been tested in model solutions containing the principle components of mining waters.

### EXPERIMENTAL

#### Materials tested

The test runs were carried out with samples prepared from channel shaped profiles of st.25 and KP-355. The chemical composition is listed in Table 1. The data summarized reveal that KP-355 has

\* To whom all correspondence should be sent.

E-mail: dimkaivanova@uctm.edu

Table 1. Chemical composition and mechanical characteristics of steels tested

Characteristics	Steels	
	KP-355	st. 25
1. Content, %		
- C	0.19	0.23
- Mn	0.65	0.54
- Si	0.4	0.4
- Cr	0.96	0.06
- Ni	0.15	0.07
- Cu	0.36	0.13
- S	0.02	0.04
- P	0.014	0.013
2. Mechanical characteristics		
- yield strength limit $R_{e, 0.2}$ , MPa	427	324
-ultimate tensile strength $R_m$ , MPa	588	503
- relative elongation $A_5$ , %	28	30

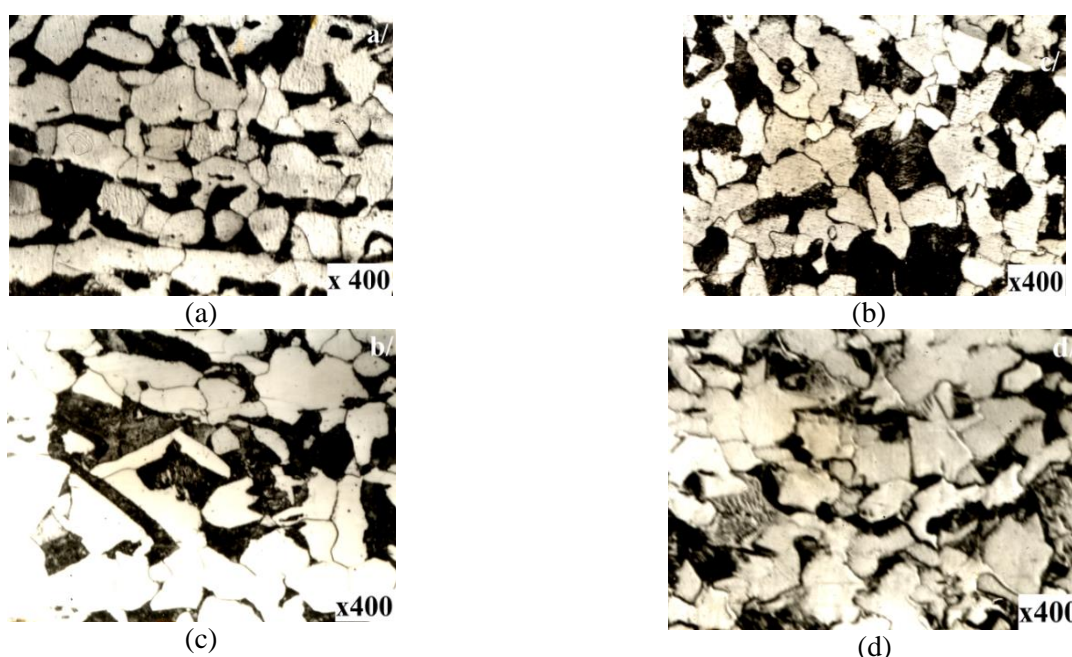


**Fig. 1** Microstructures of the steels tested: a/ – st.25, c/ – KP-355: in the hot rolling state; b/ – st. 25, d/ – KP-355: in the hot rolling state and additional 10 % deformation by strain.

greater content of chrome and copper and higher tensile strength and yield strengths, then the classical steel st.25.

The microstructures of the steels have been investigated by observations of samples prepared along the direction of rolling, using a metallographic microscope NEOPHOTE-2. The photos in Fig. 1 show the microstructures of the steels tested produced by hot rolling and after 10 % additional plastic deformation by strain. The latter is almost the same as the deformation occurring during cold deformation of the beams when they are bended. The target is to obtain a material with almost equal content but with changes in the microstructure almost close to the ones of real materials. The photos

reveal that the microstructure of both steels are almost identical, i.e. ferrite-perlite. The microstructure of st.25 has well defined strips along the direction of rolling but this effect commonly happens accidentally and cannot be related to a specific type of steel.

The changes after the additional plastic deformation in the steel microstructures are mainly in the elongations of the ferrite grains in the direction of the applied load but without any significant differences between both steels tested.

**Methods, samples, model solutions and methodology of corrosion tests**

*Polarization methods*

These methods use potentiostatic devices and are convenient for electrochemical and corrosion investigations. They allow studying actually all real relationships between the potential and the rate of the electrochemical reaction (the current density). The polarization curves, obtained by potentiostatic or potentiodynamic methods, allow many corrosion and electrochemical parameters such as  $E_{\text{corr}}$  and  $i_{\text{corr}}$  to be estimated. In addition, such tests allow the parameters of the passive state to be determined, too. A potentiostat-galvanostat PAR 273 was used in this study.

The tests were carried out in a conventional three-electrode, spatially separated, electrochemical cell with a platinum plate ( $S=2.5 \text{ cm}^2$ ) as counter-electrode. In order to avoid the transport of chloride ions from the reference electrode into the cell volume, the salt bridge was filled with the working solution.

The shape of the tested samples is cylindrical with working surface area of  $0.5 \text{ cm}^2$ . The electrodes are insulated by means of polymeric material (duracryle). The preparation of the samples includes: cleaning with glass paper № 220÷600, rinsing with distilled water and drying/degreasing with alcohol-ether mixture.

#### Model solutions

- 5 %  $\text{H}_2\text{SO}_4$ , prepared from acid (pa) and monodistilled water;
- 5 %  $\text{HCl}$ , prepared from acid (pa) and monodistilled water;
- Artificial sea water solution with the following content:  $\text{NaCl} - 26.52 \text{ g l}^{-1}$ ;  $\text{MgCl}_2 - 2.45 \text{ g l}^{-1}$ ;  $\text{MgSO}_4 - 3.3 \text{ g l}^{-1}$ ;  $\text{CaCl}_2 - 1.14 \text{ g l}^{-1}$ ;  $\text{KCl} - 0.73 \text{ g l}^{-1}$ ;  $\text{NaHCO}_3 - 0.2 \text{ g l}^{-1}$ ;  $\text{NaBr} - 0.08 \text{ g l}^{-1}$ , prepared from chemicals (pa) and monodistilled water;
- Solutions with various concentrations of the sulphate ions, prepared from  $\text{Na}_2\text{SO}_4$  (pa) and monodistilled water. The concentrations of  $\text{SO}_4^{2-}$  were:  $100 \text{ mg l}^{-1}$ ,  $500 \text{ mg l}^{-1}$  and  $2500 \text{ mg l}^{-1}$ . The pH of these solutions was varied within the range 3.0 – 9.0 by addition of either concentrated  $\text{H}_2\text{SO}_4$ , (pa) or  $\text{NaOH}$ , (pa).

#### Test protocol

The initially prepared sample (electrode) was mounted in the compartment of the working electrode in a way that the distance between it and the Haber-Luggin capillary to be about 1 mm. The counter electrode (Pt) and the bridge of the calomel reference electrode (SCE) were correctly placed in the other cell compartment.

At the beginning, prior to the records of the polarization curves, additional cathodic treatment of the sample at a potential of  $-1200 \text{ mV (SCE)}$  for 1

min was carried out. After that, the potential shifts in the positive direction with a sweep rate  $50 \text{ mV min}^{-1}$ .

The polarization curves allow determining the following corrosion-electrochemical parameters, among them: corrosion potential ( $E_{\text{corr}}$ ), corrosion current density ( $i_{\text{corr}}$ ), Tafel slopes of the anodic ( $b_a$ ) and cathodic ( $b_k$ ) curves, and the parameters of passive state such as critical potential,  $E_{\text{cr}}$ ; critical current density,  $i_{\text{cr}}$ ; passive potential,  $E_p$  and passive current density,  $i_p$ , and the transpassive potential  $E_{\text{tp}}$ .

## RESULTS AND DISCUSSIONS

### Tests in 5 % $\text{H}_2\text{SO}_4$ solutions

The results presented in Fig. 2 are potentiodynamic polarization relationships  $E, \text{V} - \lg i, \text{A dm}^{-2}$  of st.25 and KP-355 in 5 %  $\text{H}_2\text{SO}_4$  solutions obtained with a potential sweep rate of  $50 \text{ mV min}^{-1}$ . The main corrosion-electrochemical parameters are summarized in Table 2. The corrosion potential  $E_{\text{corr}}$  of KP-355 steel is  $-520 \text{ mV, SCE}$  and it is more positive than the one corresponding to st.25 steel (with higher carbon content), a fact that could be attributed mainly to the chrome content as alloying element.

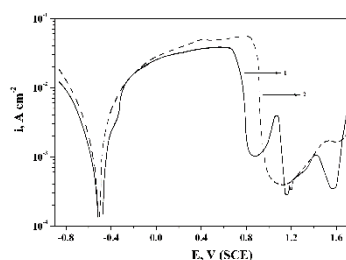


**Fig. 2.** Potentiodynamic polarization curves  $E, \text{V} - i, \text{A cm}^{-2}$ , developed in 5 %  $\text{H}_2\text{SO}_4$  solutions at  $25^\circ\text{C}$ , and non-deformed samples: (1) – KP-355; (2) – st.25.

The corrosion rate of st.25, represented by current density ( $1.2 \times 10^{-3} \text{ A cm}^{-2}$ ) is several times higher than the corrosion rate of KP-355 which could be explained by the lower carbon content and the alloying chrome and copper in KP-355 steel.

**Table 2.** Corrosion-electrochemical parameters for both steels in 5 %  $\text{H}_2\text{SO}_4$ ,  $25^\circ\text{C}$

Parameters	KP-355	st. 25
$E_{\text{corr}} (\text{SCE}), \text{mV}$	-520	-540
$i_{\text{corr}}, \text{A cm}^{-2}$	$5.6 \times 10^{-4}$	$1.2 \times 10^{-3}$
$b_k, \text{mV dec}^{-1}$	120	125
$b_a, \text{mV dec}^{-1}$	50	50
$E_{\text{cr}} (\text{SCE}), \text{mV}$	630	790
$i_{\text{cr}}, \text{A cm}^{-2}$	$1.6 \times 10^{-1}$	$2.8 \times 10^{-1}$
$E_p (\text{SCE}), \text{mV}$	770	950
$i_p, \text{A cm}^{-2}$	$2.6 \times 10^{-3}$	$9.8 \times 10^{-4}$
$E_{\text{tp}}, \text{mV}$	1500	1690
$\Delta E_p, \text{mV}$	740	510

The values of  $E_{cr}$  and  $i_{cr}$  characterizing the transition of the steels into the passive states indicate that these parameters are not so favorable for the st.25 samples (considering the transition into the complete passive state) due to the more-positive critical potential and higher critical current density. Both steels tested demonstrate big differences in the passive states. For the st.25 samples, the passive current  $i_p$  remained almost constant ( $9.8 \times 10^{-4} \text{ A cm}^{-2}$ ), while with the KP-355 sample specific peaks were observed. The later could be related to the presence of chrome as alloying element. The Tafel slopes of the cathodic ( $b_k$ ) and anodic ( $b_a$ ) polarization curves are almost equal for both steels. This actually indicates that the mechanisms of the cathodic reactions (hydrogen evolution) as well as the anodic dissolution are identical for both steels.

The effect of the 10 % cold plastic deformation on the polarization relationships in 5 %  $\text{H}_2\text{SO}_4$  solutions are shown in Fig. 3. The comparison between the corrosion-electrochemical parameters of both steels in the deformed states reveals that the 10 % cold plastic deformation does not change significantly the main parameters with respect the ones obtained with no-deformed samples. Precisely, this comment refers to: more-positive corrosion potential ( $E_{corr}$ ) and lower corrosion current density ( $i_{corr}$ ) for the KP-355 steel and consequently easier transition into the passive state, while the passive state of st.25 is more stable.

The most important difference observed in the characteristics of the deformed and non-deformed samples is in the pre-passive and passive states. The plastic deformation leads to more negative critical potentials  $E_{cr}$ , that is the passive states appears earlier, but the critical current densities  $i_c$  in such situations are greater. Moreover, the plastic deformation enlarges the area of complete passive state and reduces the current density  $i_p$ ,  $\text{A cm}^{-2}$  (see Fig. 2 and Fig. 3).

#### Tests in 5 % HCl solutions

The corrosion-electrochemical characteristics of the steels tested in 5 % HCl solutions determined by means of the polarization relationships in semi-

logarithmic scale  $E, \text{V} - \lg i, \text{A cm}^{-2}$  are summarized in Table 3. The potentiodynamic polarization curves for both steels in the deformed states are shown in Fig. 4.

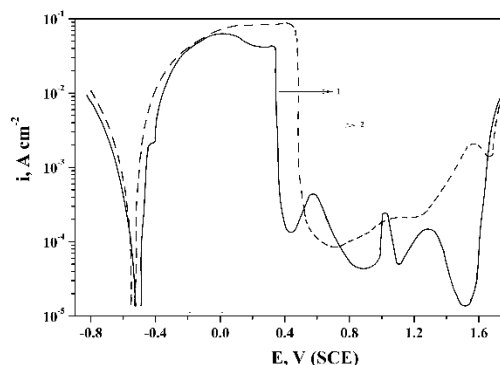


Fig. 3. Potentiodynamic polarization curves  $E, \text{V} - i, \text{A cm}^{-2}$  obtained in 5 %  $\text{H}_2\text{SO}_4$  solutions at 25°C and 10 % elongations of the steel samples:(1) – KP-355; (2) – st.25.

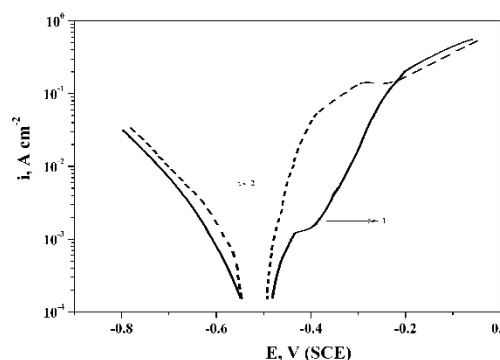


Fig. 4. Potentiodynamic polarization relationships  $E, \text{V} - i, \text{A cm}^{-2}$ , obtained in 5 % HCl solutions at, 25oC, with 10 % elongations of the steel samples: (1) – KP-355; (2) – st.25.

The corrosion rate ( $i_{corr}$ ) for st.25 in these media is of about  $1.7 \times 10^{-4} \text{ A cm}^{-2}$  and this value is significantly higher (one order higher) than the corrosion rate of KP-355 steel. In the solutions of 5 % HCl, as well as in the model media with sulphur acid content, the corrosion potential ( $E_{corr}$ ) is more-positive for the KP-355 steel that could be attributed to the copper and chrome as alloying components.

The cathodic reaction and the anodic dissolution of both steels have identical mechanisms, a standpoint supported by almost equal values of the Tafel slopes  $b_k$  and  $b_a$ .

Table 3 Corrosion-electrochemical parameters for both steels with and without 10 % cold plastic deformation, in 5 % HCl, 25°C

Parameters	Undeformed steel		10 % cold deformation	
	KP-355	st. 25	KP-355	st. 25
$E_{corr} (\text{SCE}), \text{mV}$	-370	-460	-450	-455
$i_{corr}, \text{A cm}^{-2}$	$1.7 \times 10^{-5}$	$1.7 \times 10^{-4}$	$1.6 \times 10^{-4}$	$3 \times 10^{-4}$
$b_k, \text{mV dec}^{-1}$	70	80	110	100
$b_a, \text{mV dec}^{-1}$	40	40	55	50

The cold plastic deformation does not change the corrosion-electrochemical parameters and their behaviour is similar to that in absence of deformation. However, the additional introduced energy and the effect on the steel heterogeneity leads to increased corrosion rates for both steels, mainly for KP-355, where the value of  $i_{corr}$  raises about 10 times.

*Tests in artificial sea water solutions*

In the corrosion process of both st.25 and KP-355 samples in artificial sea water oxygen depolarization take place as it well demonstrated by the polarization curves shown in Fig. 5. The parameters characterizing the corrosion behaviour are summarized in Table 6. The parameter values indicate that the dissolution rate of st.25 is higher than the one of KP-355. However, both dissolution rates are significantly lower in comparison with the ones observed in *HCl* and *H<sub>2</sub>SO<sub>4</sub>* media.

In this model solution the corrosion potential of KP-355 is more positive (with about 100 mV) with respect to the corrosion potential of st.25. The comparison of the corrosion-electrochemical parameters (see Table 4), reveals that the cold plastic

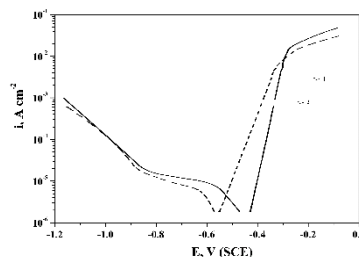


**Fig. 5.** Potentiodynamic polarization relationships E, V – i, A cm<sup>-2</sup>, obtained in artificial sea water: (1) – KP-355; (2) – st.25.

deformation does not increase the corrosion rate in contrast to the case when the tests performed in *HCl* and *H<sub>2</sub>SO<sub>4</sub>* media, but significantly reduces it. Moreover, the deformation shifts the corrosion potential of st.25 in the positive direction and makes it closer to corrosion potential of KP-355.

*Tests in aqueous sulphate solutions*

The tests with KP-355 samples, following the same methodology, produce polarization curves shown in Fig. 6.

**Table 4** Corrosion-electrochemical parameters for both steels, in artificial marine water, 25°C

Parameters	Undeformed steel		10 % cold plastic deformation	
	KP-355	st. 25	KP-355	st. 25
$E_{corr} (SCE), mV$	-520	-620	-510	-525
$i_{corr}, A cm^{-2}$	$3 \times 10^{-6}$	$4.6 \times 10^{-6}$	$8 \times 10^{-8}$	$1.2 \times 10^{-7}$
$i_d, A cm^{-2}$	$2.2 \times 10^{-5}$	$1.8 \times 10^{-5}$	$5 \times 10^{-7}$	$5 \times 10^{-7}$
$b_a, mV dec^{-1}$	40	45	45	50

**Table 5.** Corrosion-electrochemical parameters of steel KP-355 in solutions with various concentrations of sulphate ions and various pH at 25°C

[SO <sub>4</sub> <sup>2-</sup> ] mg l <sup>-1</sup>	pH	$E_{corr}, mV$ (SCE)	$i_{corr}, A cm^{-2}$	$i_d, A cm^{-2}$	$b_a, mV dec^{-1}$
100	3	-555	$2 \times 10^{-5}$	$10 \times 10^{-5}$	50
	4.5	-300	$1.88 \times 10^{-6}$	$2.6 \times 10^{-5}$	55
	5.5	-310	$2 \times 10^{-6}$	$16 \times 10^{-6}$	60
	7.5	-340	$1.3 \times 10^{-6}$	$10.2 \times 10^{-6}$	70
	9	-400	$1.1 \times 10^{-6}$	$2 \times 10^{-6}$	90
500	3	-590	$1.3 \times 10^{-5}$	$7 \times 10^{-5}$	30
	4.5	-360	$9 \times 10^{-6}$	$3 \times 10^{-5}$	55
	5.5	-380	$5 \times 10^{-6}$	$16 \times 10^{-6}$	58
	7.5	-400	$5 \times 10^{-6}$	$2.4 \times 10^{-5}$	70
2500	9	-460	$2.5 \times 10^{-6}$	$6 \times 10^{-6}$	70
	3	-600	$6.6 \times 10^{-6}$	$7 \times 10^{-5}$	29
	4.5	-460	$2.4 \times 10^{-6}$	$5 \times 10^{-6}$	39
	5.5	-410	$2 \times 10^{-6}$	$9 \times 10^{-6}$	39
	7.5	-475	$2 \times 10^{-6}$	$4.6 \times 10^{-6}$	40
	9	-450	$1.8 \times 10^{-6}$	$5.8 \times 10^{-6}$	55

These relationships were taken at concentration  $C_{SO_4^{2-}} = 100 \text{ mg l}^{-1}$  and pH in the range of 3.0 – 9.0. The plots reveal that the cathodic depolarization reaction is oxygen reduction with well-shaped oxygen levels (steps). The main parameters characterizing the corrosion of the steel tested are summarized in Table 5.

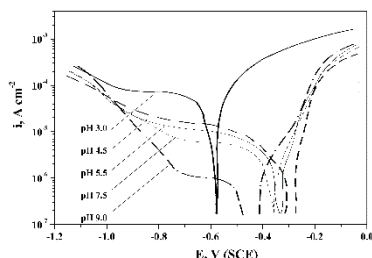


**Fig. 6.** Potentiodynamic polarization relationships  $E, V - i, A \text{ cm}^{-2}$  of KP-355 in sulphate solutions. Concentration of  $SO_4^{2-} = 100 \text{ mg l}^{-1}$  and pH 3.0-9.0 at  $25^\circ\text{C}$

The change in the corrosion potential  $E_{\text{corr}}$  with variations of pH, within the range of concentration variations are shown in Fig. 7. The values of the potentials shifts sharply from more negative (at pH=3.0) towards more positive but for pH beyond 5.0 there is a weak change in the negative direction. The plots indicate that the largest amplitude of  $E_{\text{corr}}$  appears in low-concentrated solutions ( $100 \text{ mg l}^{-1}$ ).

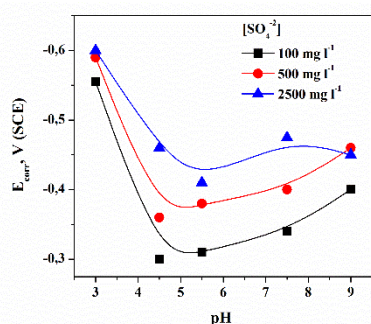


**Fig. 7.** Relationship  $E_{\text{corr}} = f(\text{pH})$  at various concentrations of  $SO_4^{2-}$  at  $25^\circ\text{C}$ .

Fig. 8 illustrates the relationship between the rates of the corrosion processes represented by the current density ( $i_{\text{corr}}$ ) as a function of the solution pH as independent variable. These plots clearly demonstrate that with increase in pH the corrosion rate initially decreases rapidly from the area of the weak (low-concentrated) solutions (pH 3.0) toward the neutral and remains almost unchanged towards the range with pH 9.0. This relationship of the corrosion rate as function of pH (beyond pH 4.5) could be explained by the fact that the cathodic depolarization reaction is oxygen reduction rather than (especially at high pH) water reduction, where corrosion rate increase with increase in the value of pH.

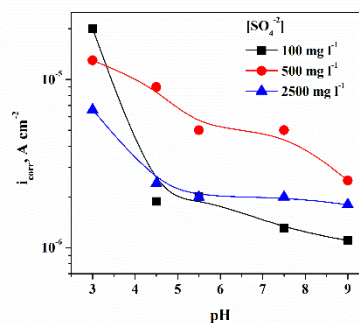


**Fig.8.** Relationship  $i_{\text{corr}} = f(\text{pH})$  at various concentrations of  $SO_4^{2-}$  at  $25^\circ\text{C}$ .

## CONCLUSIONS

The results obtained from the corrosion test with st.25 and KP-355 samples could be outlined as:

1. In model solutions of 5 %  $H_2SO_4$  the corrosion rate of st.25 is about two times higher than that of KP-355 alloyed by 0.96 % Cr and 0.36 % Cu. The registered more negative potential and the lower critical current density of KP-355 reveal that this steel demonstrate higher ability to be passive in sulphur acid media in comparison with the behaviour of st.25.

2. In model solutions of 5 % HCl the samples of st.25 dissolve more intensively with a rate of about one order of magnitude more ( $i_{\text{corr}} = 1.7 \times 10^{-4} \text{ A cm}^{-2}$ ) with respect to KP-355 where  $i_{\text{corr}} = 1.7 \times 10^{-5} \text{ A cm}^{-2}$ .

3. The corrosion rate of KP-355 steel in artificial sea water is about two times slower than the corrosion rate of st.25.

4. The corrosion potentials ( $E_{\text{corr}}$ ) of KP-355 steel in all model solutions are more positive with respect to the corrosion potentials of st.25 and this indicates better corrosion behaviour of KP-355 in aggressive media.

5. It was established that the dissolution rate  $i_{\text{corr}}$  for both steels tested increases after additional 10 % cold plastic deformation. This effect is stronger with samples of KP-355.

6. It was estimated the effect of concentration of  $SO_4^{2-}$  (100; 500 and  $2500 \text{ mg l}^{-1}$ ) and pH (3.0 ÷ 9.0) of  $Na_2SO_4$  solutions on the corrosion behaviour of KP-355 steel. The corrosion rate, irrespective of the solution concentrations, reduces rapidly from the area of weak acid solutions towards the neutral ones and remains unchanged up to pH=9.0. The shift of  $E_{\text{corr}}$  in the positive direction with increase in pH is more pronounced in the weak (low-concentrated) solutions.

#### REFERENCES

1. Gurdeep Singh, *Int. j. of mine waters*, **5**, 21 (1986).
2. Parlapanski M., *Koroziiai zashtita na sarorageniata w kamenovaglenite rudnici u nas*, Nauka, 1988.
3. Mishra B, Pak J., *ASM Handbook Volume 13C, Corrosion: Environments and Industries*, 1076 (2006).
4. Farinha P., *Biocorrosion in the mining industry - big tanks and big pipes*, ACA Symposium on Microbial Influenced Corrosion, 10-11 August, Perth, 2011.
5. Roberge P., *Handbook of corrosion engineering*, McGraw-Hill, New York, 1999.
6. Gasior O., Farinha P., *Corrosion & Prevention*, **90**, 6 (2013).
7. Gray W., Harrison G., Farinha P., Risbud M., *Financial benefit to a corrosion aware mine site culture*, *Corrosion & Prevention*, Paper **118**, 1(2015).
8. Hassell R., Villaescusa E., Thompson A., and Kinsella B., *Corrosion assessment of ground support systems*, *Proceedings of 5th International Symposium on Ground Support in Mining and Underground Construction*, Perth, Australia, (2004).
9. Wu S., Northover M., Craig P., Canbulat I., Hagan P., Saydam, S., *Environmental influence on mesh corrosion in underground coal mines*, *Int. j. of mining, reclamation and environment*, Published online: 13 Mar 2017, p. 1-17.
10. Duprat M., Bar N., Dabosi F., *J. Appl. Electrochem.*, **8**, 455 (1978).
11. Meyer D., Heinrich L., Reinhard D., *Korrosion*, **17**, 211(1968).
12. Bonel A., Dabosi F., Deslois C., Duprat M., *J. of Electrochem. Soc.*, **130**, 753 (1983).
13. Kowaka M., Ayukava M., Nagano N., *Sumitomu Kunsoki*, **21** № 2, (185) 1969.

### КОРОЗИОННО ПОВЕДЕНИЕ В МОДЕЛНИ РАЗТВОРИ НА СТОМАНИ, ПРЕДНАЗНАЧЕНИ КАТО КОНСТРУКЦИОННИ МАТЕРИАЛИ ЗА МИННАТА ИНДУСТРИЯ

Д. И. Иванова\*, Г. П. Илиева, Л. Б. Фачиков

*Химикотехнологичен и металургичен университет, бул. „Кл. Охридски” 8, София 1756, България*

Постъпила на 15 ноември 2017 г.; приета на 12 декември 2017 г.

(Резюме)

Извършено е сравнително изследване на корозионното поведение на две стомани, предназначени за руднично крепене: широко използваната въглеродна стомана ст.25 и новопредлаганата, нисколегирана стомана КР-355 (0.96% Cr, 0.36% Cu). Изпитванията са проведени в моделни среди, подбрани така, че да съдържат основните агресивни компоненти в повечето реални руднични води. С помощта на физични и електрохимични методи за изследване и анализ, са определени най-важните параметри, характеризиращи механичните свойства и корозионно-електрохимичното поведение на стоманите. Установено е, че стомана КР-355 е с по-добри якостни показатели и като цяло се отличава с по-висока корозионна устойчивост във всички използвани моделни среди.

**Ключови думи:** корозия, въглеродни и нисколегирани стомани, руднични води